euronoise

Nonlinear propagation of spark-generated N-waves in atmosphere: theoretical and experimental assessment of the shock front structure

Petr Yuldashev[a], Mikhail Averiyanov[a], Vera Khokhlova[a], Oleg Sapozhnikov[a,a], Ollivier Sebastien[b] and Philippe Blanc-Benon[b]

[a]Center for Industrial and Medical Ultrasound, Applied Physics Lab., University of Washington, 1013 NE 40th St., Seattle, WA 98105, USA
[b]Ecole Centrale de Lyon, LMFA, UMR CNRS 5509, Ecully, 69134 Lyon, France
petr@acs366.phys.msu.ru

Extensive outdoor and laboratory-scale experiments on sonic boom propagation in turbulent atmosphere have shown that shock wave amplitude and rise time are important parameters responsible for sonic boom annoyance. However, accurate measurement of the shock front structure with standard microphone remains a challenge due to the broadband spectrum of the *N*-wave shock front. In this work the experimental setup utilizing a spark source has been designed and built to investigate nonlinear *N*-wave propagation in homogeneous air. Short duration (30 μs) and high amplitude (1 kPa) spherically divergent *N*-waves were generated. In addition to acoustic measurements with 1/8" B&K microphones, the shadowgraphy method using short duration flash lamp (20 ns) and CCD camera was employed to assess the shock front structure at different distances from the spark. It was shown that the shock rise time measured by the shadowgraphy method was in a good agreement with the theoretical predictions and it was 10 times shorter than in the microphone measurements. The widening of the shock in acoustic measurements was therefore due to the limited bandwidth of the microphone. The combination of modeling, acoustic, and optical measurements provided an accurate calibration of the shock wave measuring system. [Work supported by RFBR and INTAS.]

1 Introduction

Development of civil supersonic transport motivates theoretical and experimental studies of shock wave propagation in the atmosphere [1-4]. Intensive shock waves generated by supersonic aircraft propagate in the turbulent atmosphere towards the ground. Due to strong nonlinear effects the initial waveform transforms to the shape of an *N*-wave. Focusing and defocusing at turbulent inhomogeneities result in formation of an acoustic field with nonuniform acoustic pressure distribution. The signal on the ground is an impulsive noise for people. High pressure level leads to high noise loudness and increasing annoyance and may affect human being. In addition to pressure level, an important characteristic of shock wave is a rise time that is defined as the time for the pressure to increase from $0.1P_{max}$ to $0.9P_{max}$. It has been shown that subjective loudness increases with decreasing of the rise time [3]. To estimate possible noise effect the predictions of characteristics such as peak and average pressure, pulse duration and shock rise time are required. Complete theoretical investigation of nonlinear *N*-wave propagation is a complicated problem. Most of the theoretical results have been obtained up to date within the simplified models like geometrical acoustics and parabolic approximation [2].

Experimental studies of real *N*-wave propagation are difficult due to the high costs and unsteadiness of turbulence characteristic and other atmospheric parameters during outdoor propagation measurements. The experimental efforts therefore have turned to the laboratory-scaled measurements that have been shown to be a good alternative to the field experiments [4, 5]. An electrical spark source can be used to generate shock waves and plane jet - to produce kinematical turbulence. Since the turbulent fields and the sources are better controlled in laboratory environment, it gives an opportunity for more accurate investigation on how turbulence parameters affect the properties of the acoustic field. Laboratory-scaled experiments can be also used to validate different theoretical models that would be applied to govern *N*-wave propagation in real atmosphere.

In a laboratory-scaled experiment performed in LMFA, electrical spark source was used to generate spherical acoustic *N*-wave with the amplitude of 1000 Pa and duration of 30 μs at 15 cm from the source [5]. High frequency and wide band microphones (*Bruel & Kjær*) of 1/8 inch diameter were used in experiments without a grid

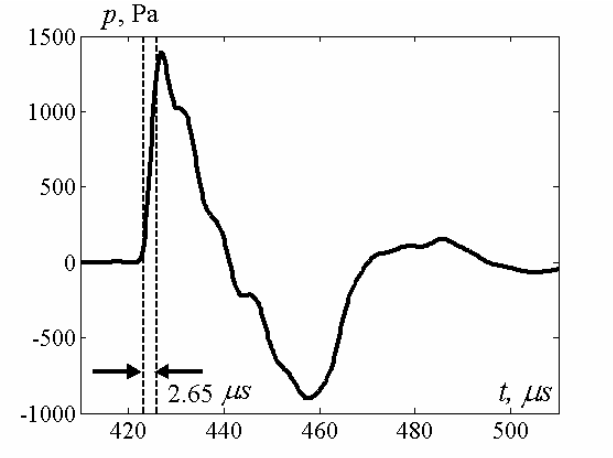

Fig.1 Experimental *N*-wave wave measured at 15.8 cm from the spark source.

to avoid diffraction effects on it. The microphones were mounted in a baffle in order to postpone the diffracted waves. *N*-waves passed through kinematical or thermal turbulent layer were measured and statistical results for peak positive pressure and rise time were presented. Strong variations of peak positive pressure and rise time were observed in the presence of turbulence. In many cases peak pressure up to 5 times the value recorded without turbulence were detected. Peak pressure levels lower than in a quiet air were also observed and have significant occurrence probability greater than 50%. It was shown that the mean rise time increased with the turbulence intensity, and observed rise time in the presence of turbulence can be several times longer but not much shorter than without the turbulence. One of the important results is that the measuring system could not measure sufficiently short rise times. This conclusion was made based on the experimental data analysis. It appeared that in turbulent medium measured rise times were not shorter than in still medium, whereas according to the theoretical predictions very steep shock fronts should be observed in focusing zones. This discrepancy between the measured and expected values of the shortest rise time was attributed to insufficient frequency band of measuring system setup which includes the *Bruel & Kjær* microphone having 140 kHz cut-off frequency as provided by the manufacturer.

To better understand the effect of the spectral characteristics of the microphone on measured rise time, *N*-wave propagation through homogeneous air was studied theoretically and experimentally [7]. *N*-waveforms were measured at different distances from the spark source and

compared with the results of numerical simulations based on the Burgers equation extended to include relaxation processes and spherical divergence of nonlinear wave. Numerical and experimental results were shown to be in a good agreement only after applying a microphone

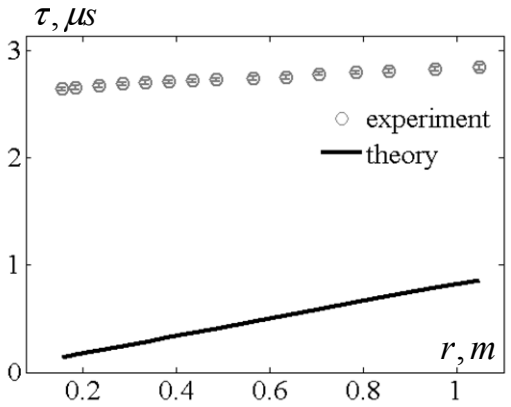

Fig.2 Comparison of measured by the microphone (circle markers) and theoretically predicted (solid line) rise time without applying microphone frequency response.

amplitude frequency response to the theoretically obtained waveforms. A typical experimental waveform recorded at 15.8 cm from spark is shown in Fig.1. Front rise time equals to 2.65 μs and is marked by two vertical dashed lines. In Fig. 2, experimental rise time is compared to the theoretical values calculated without applying the microphone response. Theoretical results (solid line) were obtained for the propagation of the initially symmetric *N*-wave of 1400 Pa amplitude at 15.8 cm from the source, that corresponds to the experiment. Air conditions were chosen close to those measured during the experiment. It is seen that experimental rise time is only about 2.7 μs and almost does not grow with the propagation distance. In contrast, theoretical rise time is ten times shorter than experimental and increases from 0.15 μs at closest distance 15.8 cm to 0.85 μs at 105 cm. To prove theoretical predictions an optical experimental setup, which allows visualizing acoustic wave shock front and *a priory* has better resolution than acoustic measurement setup, was installed.

2 Optical visualization of shock front

2.1 Experimental method

Two main visualization techniques of transparent inhomogeneities in continuous media are used: schlieren and shadowgraphy methods [8]. In this work a shadowgraphy method is proposed as an alternative to acoustic measurements with a goal to resolve the shock front structure. An image in the shadowgraphy method is formed due to refraction of light on inhomogeneities of the refraction index of the propagation medium, which in our case are governed by the passing acoustic wave. Refraction of light leads to intensity redistribution in an observation plane. The advantages of shadowgraphy method in comparison with schlieren are relative simplicity and lower requirements to the elements of optic system [8]. One disadvantage of shadowgraphy method is that the shadow image scale does not correspond exactly to the scale of considered transparent object, and magnification of the image depends on the distance between this object and the observation plane. In addition, the object is inherently three dimensional but the image is only two dimensional. These circumstances complicate quantitative analysis of object properties. However a model that governs ray refraction at the object and describes the image formation can be built to reconstruct the object dimensions. One more disadvantage is that shadowgraphy is characterized by lower sensitivity than schlieren. However, since sufficiently strong shock waves producing large refraction angles are considered, this method can be employed.

2.2 Experimental setup

The experimental arrangement for visualizing the structure of the *N*-wave shock front is schematically represented in Fig.3 (view from above). It generally consists of two main parts: optical and acoustical, connected with a synchronization system. Optical part basically includes a flash-lamp (*Nanolite* KL-L model, 3.5 kV tension), light filter, lens (4 cm diameter, 16 cm focusing length), digital camera (*Dantec dynamics*) with acquisition system, *Nikon* objective, and calibration grid. Acoustical part includes a 15 kV spark source (15 mm gap between tungsten electrodes), 1/8 inch *Bruel & Kjær* microphone mounted in a baffle, preamplifier, amplifier (*Bruel & Kjær, Nexus*), and acquisition system. Elements of the setup are mounted on two perpendicular rails, one for optical and one for acoustical part.

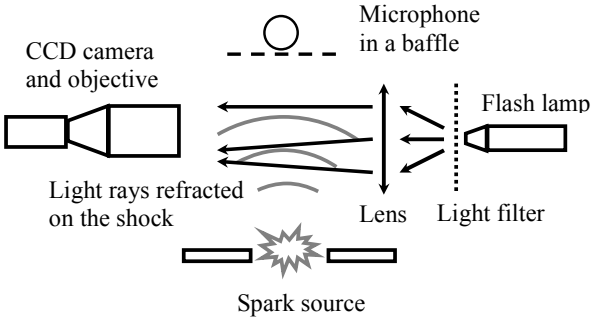

Fig.3 Diagram of experimental setup, view from above.

A flash-lamp contains a small-size spark source which is used to generate white light flashes with duration about 20 nanoseconds. Having short duration light flashes is necessary in the experiment as soon as according to theoretical estimations, the minimum measured rise time is as small as 0.1 μs. A flash light is collimated by the focusing lens to produce a parallel beam which after passing through the acoustic shock front is collected by the objective. The objective is mounted together with the CCD camera. The resolution of the camera is 1600 pixels in the horizontal coordinate along *N*-wave propagation direction and 1186 pixels in the vertical coordinate. A light filter was used to reduce the amount of light in the image to avoid the damage of the CCD matrix. The *Nikon* objective has the focal distance 60 mm. Optical instruments were aligned coaxially. A spatial grid uniformly filled by small black circles was used to measure the image spatial scale in pixels per cm. A distance between the centers of circles was 0.5±0.005 mm. The image of the grid was also used to

control the distortions possibly introduced by the optical system.

Optical and acoustical parts of the experimental setup are connected with the synchronization system. The measurements are triggered by the electromagnetic signal produced by the electric discharge of the acoustic spark source and received by an antenna connected to one of the oscilloscope channels. As each part of the measurement setup has its own internal delay between receiving the TTL signal and triggering, two synchronization signals were used, one for optical setup and the second for acoustical setup. This ensures precise measurements of the same acoustic shock front. To compensate *N*-wave propagation time from the source to the area illuminated by the parallel flash light beam the generator introducing corresponding time delay to the synchronization signal was used (long scale, hundreds of μs, gross adjustment). This signal was used to trigger the acoustic acquisition system. Optical setup needs finer time adjustment of synchronization signal. For this purpose additional delay line was used, which is also responsible for compensating the internal delay of the camera before triggering (190 μs). Thus, triggering of the optic measurement system was changed with the time step of 1 μs.

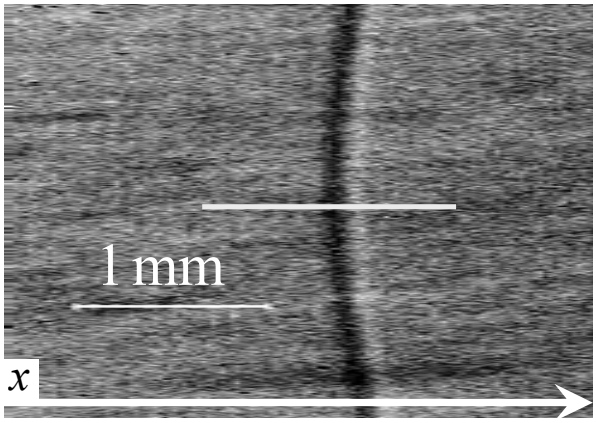

Fig.4 Typical shadowgraphy image of the shock front.

3 *N*-wave shock front structure

3.1 Theoretical model

Optical and acoustic measurements of the shock front were performed at different distances from 15 cm to 60 cm between the optical axis and the spark source. The shortest distance was limited by the microphone saturation and its possible damage due to very high pressure amplitudes. The longest distance was limited due to the low image contrast as the amplitude of spherically divergent wave rapidly decreases with distance and shock rise time increases. The refraction angles and therefore light redistribution become smaller. The typical image of the shock front is presented in Fig. 4. The shock propagates in the negative direction of the *x* axis, producing the vertical line in the image. Slight curvature of the shadow image is observed due to the spherical geometry of the wave front. The shock front shadow image has nonuniform structure with dark and light stripes. Series of images with a different position of the objective focus along the light beam were recorded for each distance. Analysis of the series shows that the contrast and thickness of the shadow stripe change with the focal plane position. Lower contrast corresponds to lower thickness of the stripe. This behavior is typical for shadowgraph image. The further optical rays propagate from the inhomogeneity, the stronger they diverge or converge. Strong divergence and convergence of optical rays amplify redistribution of light intensity, which is directly related to the image contrast. Refraction angles also increase with distance that results in larger image of the object. The size of shadow thus does not correspond to the real object size. Geometrical optics is used here in order to govern the formation of an image.

A schematic diagram of mutual position of an incident light beam and refraction index inhomogeneity produced by the shock front is shown in Fig.5. Since shock front in the image is almost a straight line, except for a slight curvature, a two dimensional model is used here to simplify calculations. A spatial distribution of refractive index of the shock is modeled as a hyperbolic tangent function:

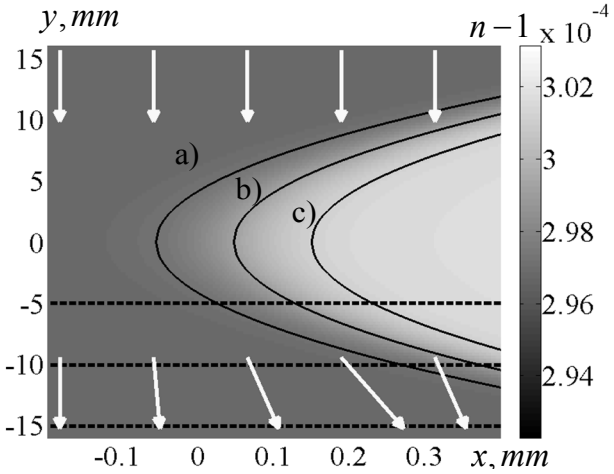

Fig.5 Two dimensional spatial distribution of refractive index induced by the shock front. Three solid lines show levels a) 0.1, b) 0.5 and c) 0.9 from Δn_{sh}. Three dashed lines correspond to observing planes used in Fig. 6. White arrows schematically represent directions of light rays.

$$n = n_1 + \frac{\Delta n_{sh}}{2}\left[\tanh\left(\frac{r - r_0}{a}\right) + 1\right]. \qquad (1)$$

Here n_1 is the refractive index of a quiet air, Δn_{sh} is the variation of refractive index on the shock following the pressure increase from zero to the wave pressure maximum, r_0 is the shock front position relative to the spark source, a is the characteristic spatial thickness of the shock. The relationship between the shock thickness a and the rise time τ for hyperbolic tangent shape of the shock is $a = c_0\tau/2.2$. The proposed spatial distribution of the refractive index, Eq.(1), is in accordance with theoretical predictions based on Burgers equation. The system of geometrical optics equations can be written in a Hamilton-Jacoby formulation [9] as:

$$\frac{d\mathbf{r}}{d\theta} = \mathbf{p} \quad ; \quad \frac{d\mathbf{p}}{d\theta} = \frac{1}{2}\nabla n^2 . \qquad (2)$$

Here vector **p** represents a gradient of eikonal and shows the direction of the light ray, vector **r** represents a trajectory of the ray, the parameter θ determines the propagation path along the ray. Initial conditions correspond to parallel beam incident from the negative direction of the y axis. These equations were solved numerically using the fourth order accuracy Runge-Kutta algorithm. Light intensity in observation plane was calculated as inversely proportional to the cross-sectional area of the light ray tube. Intensity images were analysed at different distances from the line of shock symmetry $y = 0$.

In order to develop a criterion of the acoustic shock front rise time estimation on the basis of the light propagation model, the changes in shadow image due to variation of peak pressure $P_{\max}$ and rise time τ were analysed. According to the acoustic measurements of peak pressure and theoretical estimations for the rise time, peak pressure $P_{\max}$ varied within the interval from 500 to 2500 Pa and rise time τ from 0.1 to 1.0 μs. The relationship between the refractive index n and wave pressure P' is linear

$$n = 1 + k(\rho_0 + P'/c_0^2), \qquad (3)$$

where the constant k = 0.00023 m^3/kg. A typical shadow intensity distribution is shown in Fig.6 for $P_{\max}$ = 1000 Pa, τ = 0.2 μs and three different distances y = -5 mm, -10 mm, and -15 mm. The vertical dash line indicates the position of shock centre and two solid vertical lines indicate the levels of 0.1 and 0.9 from the maximum of refractive index. Similar to the experiment, intensity distribution is a combination of dark (where $I/I_0<1$) and light (where $I/I_0>1$) zones. It is shown that for considered values of $P_{\max}$ and τ, the ratio of the front width $c_0\tau$ and the distance between the maximum and minimum intensity is about 1.31 for

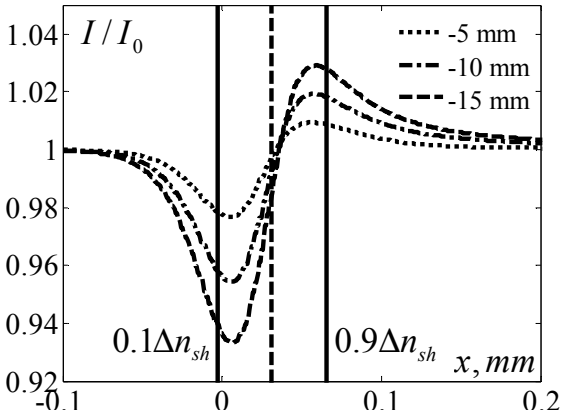

Fig.6 Intensity distribution for three positions of the observation plane: y = -5 mm, -10 mm, and -15 mm.

distances closer than 1.5 cm to the plane of symmetry y=0. At few cm from y = 0 plane diffraction effects can affect to image because for strong shock geometrical optics predicts caustics formation. For rise time, therefore, estimation only those images were used, for which focal plane lies not further than 1.5 cm from the plane y = 0.

3.2 Experimental results

To improve signal-to-noise ratio in optical images of shock fronts (an example in Fig.4), the images needed to be processed. Shown in Fig.7 is the intensity distribution along one horizontal image string in Fig. 4 (gray solid line). Intensity distributions were averaged along the vertical coordinate because the thickness of the shock did not change with the vertical coordinate, only curvature of the front was observed. It is seen that the averaging procedure results in significant reduction of noise (Fig. 7 dashed line). Before averaging it was necessary to eliminate the curvature of the line to prevent superposition of the dark and light areas.

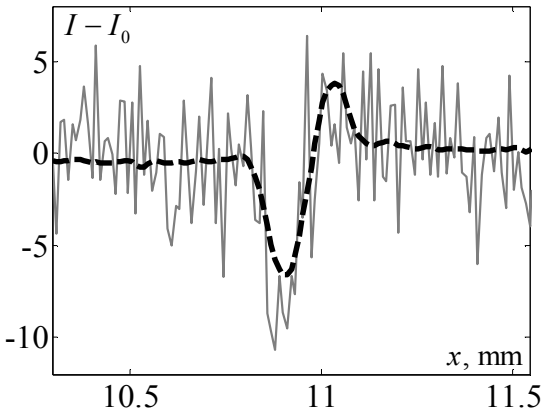

Fig.7 Comparison of averaged (dash line) and single string (solid gray line) signals.

Using six hand marked points at the shock front, the radius and the center of curvature were calculated and all strings of image were shifted to obtain vertical non curved line. Note that the center of the curvature appeared to be in a good agreement with the acoustic source spark position. Signals in Fig 7 are symmetric around zero, because the background light level I_0 was subtracted from the images to make automatic signal processing possible. The distance between the maximum and minimum intensity was measured and the rise time was calculated as $\tau = 1.31\Delta x/c_0$. Fifteen images captured in the same conditions were used to supply additional averaging.

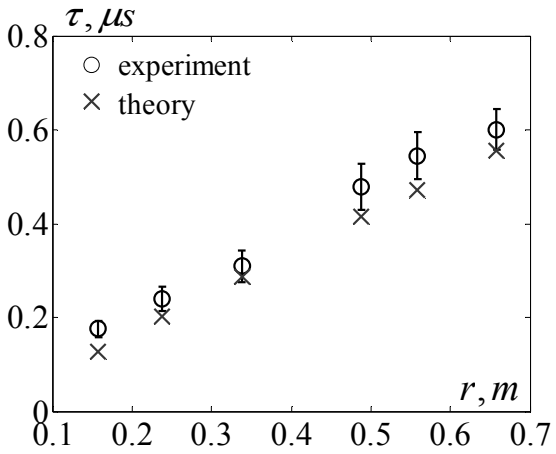

Fig.8 Comparison between the optical measured rise time (circle markers) and theoretically calculated (cross markers) at different distances from the spark source.

The results are shown in Fig.8. Round markers correspond to the measured rise time. Cross markers are the theoretical rise times calculated based on the Burgers-type equation for the N-wave with initial amplitude of 1390 Pa at

the distance r = 15.8 cm [7]. Theoretical values are not presented as a continuous curve because each experimental point was measured in slightly different atmosphere conditions (air humidity and temperature), which was accounted in simulations for each point. It is seen that theory and experiment are in a good agreement. The largest discrepancy is observed for the narrowest shock at the shortest distance of 15.8 cm from the spark source. For other distances, the difference does not exceed 15 %. It is seen that experimental points are always presented higher than theoretical. This can be the result of still insufficient sensitivity of the experimental shadowgraphy method. Limitations of geometrical optics may also play some role because diffraction effects were neglected in calculations.

4 Conclusions

Optical measurements permitted to resolve the shock front structure contrary to the microphone measurements. Shock rise time measured using the optical method is in a good agreement with the theoretical predictions and represents the same growing dynamics while the *N*-wave propagates from the source. Bandwidth limitations of the acoustic measurement setup therefore were shown experimentally. Schlieren method could be employed in further experiments to obtain more precise results of optical measurements. Advanced experiment using schlieren technique is interesting in a context of a recently proposed calibration procedure of the microphones [7]. More precise information about shock front structure would improve the calculation of spectral characteristics of the measuring system obtained as a ratio of the measured and theoretically predicted signal spectra.

Acknowledgments

This work is supported by RFBR and INTAS grants.

References

[1] K. J. Plotkin, "State of the art of sonic boom modeling", *J. Acoust. Soc. Am*., 111(1) Pt 2. 530-536 (2002).

[2] Ph. Blanc-Benon, B. Lipkens, L. Dallois, M.F. Hamilton, D.T. Blackstock. "Propagation of finite amplitude sound through turbulence: modeling with geometrical acoustics and the parabolic approximation", *J. Acoust. Soc. Am*. 111(1). Pt 2. 487-498 (2002).

[3] D. Leatherwood, B. M. Sullivan, K. P. Shepherd, D. A. McCurdy. "Summary of recent NASA studies of human response of sonic booms", *J. Acoust. Soc. Am*. 111(1) Pt 2. 586 – 598 (2002).

[4] B. Lipkens, D.T. Blackstock, "Model experiment to study sonic boom propagation through turbulence. Part I: Model experiment and general results", *J. Acoust. Soc. Am.* 103(1). 148-158, (1998).

[5] S. Ollivier, Ph. Blanc-Benon, "Model experiment to study acoustic N-wave propagation though turbulence", *AIAA-2004-2921, 10th AIAA/CEAS Aeroacoustics Conference, Manchester, United Kingdom, May* 10-12, (2004).

[6] B. Lipkens, D.T. Blackstock, "Model experiment to study sonic boom propagation through turbulence. Part II: Effects of turbulent intensity and propagation distance through turbulence", *J. Acoust. Soc. Am*. 104(3). 1301-1309, (1998).

[7] P.V. Yuldashev, M.V. Averiyanov, V.A. Khokhlova, S. Ollivier, Ph. Blanc-Benon, "Nonlinear spherically divergent shock waves propagating in a relaxing medium", *Acoust. Phys*., 54(1), 32–41 (2008).

[8] G.S. Settles, "Schlieren and shadowgraph techniques, Visualizing phenomena in transparent Media", *Springer-Verlag, Heidelberg*, (2001).

[9] Y. A. Kravtsov, Y.I. Orlov, "Geometrical acoustics of inhomogeneous medium", Moscow «*Nauka*», (1980).